Large Scale Wind Resource Mapping Using a State-of-the-Art 3D Scanning Lidar

Stephen Hannon, Keith Barr, John Novotny
Lockheed Martin Coherent Technologies
Lafayette, Colorado United States
steve.hannon@lmco.com

Jeremy Bass, Andrew Oliver, Mike Anderson
Renewable Energy Systems Group
United Kingdom, United States
jeremy.bass@res-ltd.com

Abstract:

Lockheed Martin and Renewable Energy Systems (RES) have recently undertaken groundbreaking evaluations of large-scale wind flow mapping using a scanning pulsed Doppler lidar device. Unlike sodar and short-range lidar devices, which measure wind profiles at a single location, the 3D scanning lidar can return accurate wind profiles over a large geographic area at high resolution. This paper presents measured results from a month-long campaign at a large site, including cross-comparisons with mast anemometer data. The data are intriguing and show significant promise relative to the challenging wind resource characterization problem facing wind farm developers.

Keywords: wind, remote sensing, lidar, wind energy, wind resource characterization

1 Introduction

Wind farm development in the burgeoning renewable energy market is not without its challenges. Key among these is accurate wind resource characterization. Today, two to three instrumented towers are typically placed on a prospective site to collect one to two year's worth of data. These data help validate and augment model predictions factoring in terrain profiles, prevailing wind conditions, boundary conditions, and other parameterizations. Sodar and emerging short-range lidar sensors can provide local wind profile data in support of these endeavors, though their use is not widespread. Because these sensors make measurements up to 150 to 200 m, they can cover the height range of interest to modern-day wind turbines. However, they are limited to observations of a single horizontal location per sensor. A more desirable approach would be to generate wind profiles over a very large geographic area, of the order of 10 km, at high resolution. This would enable potentially large sites to be mapped quickly and comprehensively, with the real-world effects of steep slopes and forestry measured directly, rather than inferred through modeling.

Commercial pulsed Doppler lidars have been installed in numerous environments and applied to a wide range of wind and aerosol sensing problems [1], [2]. Wind shear and turbulence monitoring at airports requires Doppler lidars having the capability to reliably measure winds to distances of 8-10 km or more. The WindTracer® is just such a device. Over the past half dozen years, consistent, reliable performance has been demonstrated by WindTracer Doppler lidar systems installed and operating around the clock at Hong Kong's International Airport, Tokyo Haneda Airport, Paris Charles de Gaulle Airport, and several other airports and sites around the world. The question arises as to how well this same technology can be applied to meet wind resource characterization challenges that face wind farm developers today.

To begin answering the above question, RES sponsored a month-long data collection and validation campaign with a WindTracer system at a prospective wind farm site in the United States. The results of this campaign have been very positive and intriguing. This paper provides a brief description of the WindTracer Doppler lidar and the data collection effort. Sample results are presented along with cross-comparisons between the lidar-derived winds and mast anemometer data.

2 System Description

Figure 1 shows a picture of a typical WindTracer system mounted on a trailer for local transport. The system operates at an eyesafe infrared wavelength of either 2 μm or 1.6 μm. For the data collection campaign described herein, a 2 μm system was utilized.

The system transmits 1-2 Watts of average power, yet it is able to make measurements to distances of 8-12 km. This range performance is achieved because the peak transmit power is ~4 kilowatts or more per pulse and the receiver employs photon-sensitive coherent heterodyne detection of the return radiation.

Figure 1: Trailer-mounted WindTracer pulsed Doppler lidar.

Figure 2 illustrates the system principle of operation. WindTracer transmits pulses of invisible, eyesafe infrared laser radiation to scatter off naturally-occurring dust or aerosol particles. Some 500-750 pulses are transmitted per second. The particles move with the wind and induce a frequency change in the return echo. This frequency change is detected by the onboard signal processor and is directly related to the wind along the scanner look direction. Time gating of the return signal enables 100 or more ranges to be simultaneously measured at each update, with range resolution of 40-100 m, depending in the system transmit pulse duration and processing configuration. Under automatic computer control, the system scans the transmit beam through up to 360 degrees in azimuth and through multiple elevation tilts to provide 3D volumetric coverage. Scan strategies are tailored to meet customer and site requirements, as described later in this paper. Data products are produced and archived, displayed locally and/or broadcast to other locations. The environmental equipment shelter housing the equipment is connected to remote operator stations via an Ethernet connection.

One of the major benefits of WindTracer is its ability to scan near obstacles and the ground without concern for side lobe clutter interference. Therefore, remote sensing of winds in the wind-energy-critical 40 to 200 m height regime is readily achieved. Side lobe clutter is a significant challenge for microwave radar devices and essentially precludes their use for this application.

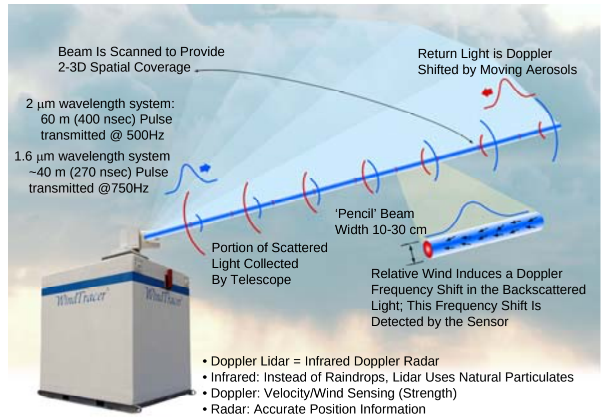

Figure 2: Pulsed Doppler LIDAR principle of operation.

Table 1 provides a summary of WindTracer system parameters. Two columns are included: one for the 2 μm system utilized during this field campaign, and one for the newer 1.6 μm wavelength configuration. This next generation system has been introduced in the latter half of 2007 and operates at a wavelength of 1.6 μm with an average transmit power of ~2W [3].

Parameter	2 μm System Configuration	1.6 μm System Configuration
Transmit Wavelength	2022 nm	1617 nm
Average Power	1 W	2 W
Pulse Energy	2 mJ	2-5 mJ
Pulse Repetition Frequency	500 Hz	200-1000 Hz
Pulse Duration	400 ns (60 m)	200-300 ns (30-45 m)
Aperture Diameter	>10 cm	>10 cm
Maximum Wind Speed	0 - 22 m/s, 0-40 m/s option	0 - 38 m/s standard
Maximum Range	8-10 km	8-12+ km
Velocity Accuracy	0.1 to 0.5 m/s	0.1 to 0.5 m/s
Output Grid Spacing	100 m typical, 10 m vertical	100 m typical, 10 m vertical

Table 1: WindTracer System Specifications

Figure 3 is a picture of the new transceiver and control electronics. The significantly shorter pulse duration of the 1.6 μm system enables higher spatial resolution wind measurement. In addition, the core subsystems have been reduced in size by a factor three, which allows compact system packaging schemes to be considered.

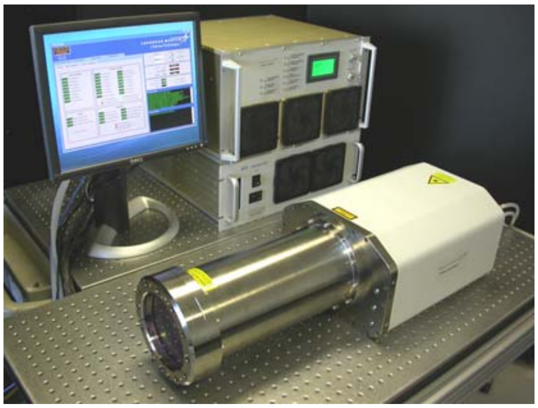

Figure 3: Next Generation 1.6 μm transceiver and transceiver control unit.

2.1 Scan Strategies

Flexible coordinate-based scan strategies are utilized to best meet wind resource characterization needs for a particular site. A two-axis scanner slews the beam through multiple large-azimuth swaths and elevation tilts. Volume scan are typically completed within 5-10 minutes. With individual line-of-sight radial velocity estimate update rates of 5 Hz or more, requirements associated with spatial resolution in both height and horizontal distance dictate the specifics of the scan. Vector wind estimates over the output grid are produced for each volume update.

Site-specific measurement requirements govern whether the lidar is centrally-located or offset to the side. Figure 4 illustrates these configurations relative to a general region of interest (ROI). A centrally-located lidar site has the advantage of reducing the distance to any measurement point in the ROI. The angular extent of the radial velocity data used to estimate the vector velocity at each point on the grid is also maximized with this approach. One potential disadvantage of the centrally-located sensor is the 250-300 m 'blind spot' that surrounds the pulsed lidar. This blind spot arises during, and for a short time after, the transmission of each pulse of radiation. Another potential disadvantage is that the number of elevation tilts needed to access the desired heights over the ROI tends to be higher for the centrally located sensor. These trades were evaluated for the short-duration campaign highlighted in this paper, and it was determined that the centrally-located sensor configuration was the most appropriate.

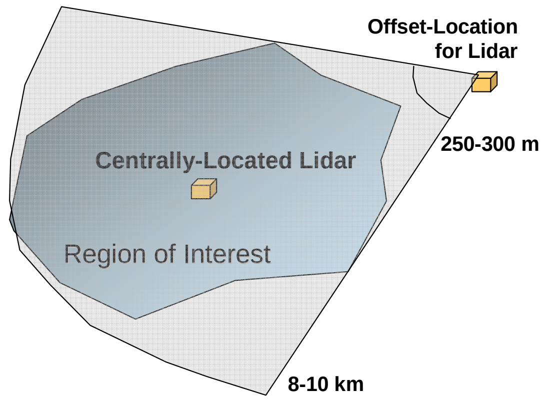

Figure 4: Centrally-located or offset-sited lidar configuration selected to best meet measurement requirements. Scan strategies are adjusted accordingly. The 2007 measurements utilized a centrally-located WindTracer.

2.2 Radial Velocity Data and Vector Wind Retrieval

Radial velocity estimates for each of ~100 range gates distributed over ~10 km are produced at an update rate of 5-10 Hz as the scanner executes the volume scan. Radial velocity accuracy of 0.1-0.5 m/sec (depending on the SNR level) is achieved. The radial velocities are then processed to produce vector velocity estimates based on a set of data distributed in angle and range around the point of interest. Figure 5 shows a sample wind velocity map for data collected at an airport in Colorado with a 2 μm wavelength WindTracer system. Velocities are plotted as standard wind barbs on top of the color-coded radial velocity estimates.

Radial velocity estimates are converted to vector wind using a localized least-squares approach similar to Volume Azimuth Processing (VAP) for radars. More sophisticated vector retrieval techniques can and have been applied to WindTracer data, such as Variational Assimilation (VAR) processing [4]. The vector wind estimates are then adjusted to correspond to a constant height above ground. This approach benefits turbine micrositing because variation in the winds over the ROI is rendered at a constant, relevant AGL height or set of heights. Data slices produced at multiple heights can then provide direct insight into shear effects, including low-level jets.

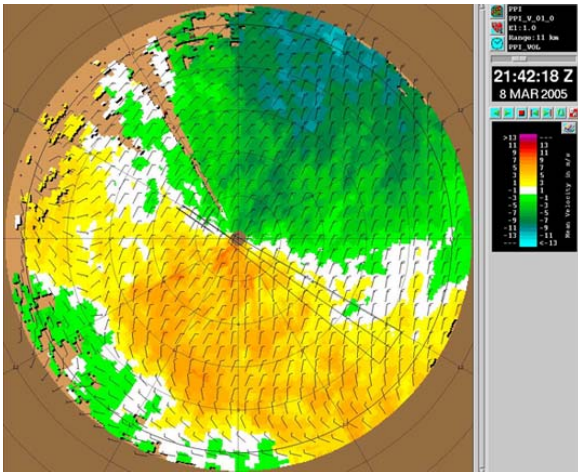

Figure 5: Sample WindTracer color-coded radial wind velocity map at a 1 degree elevation tilt and out to a maximum range of ~11 km. Overlaid on the radial velocities are wind barbs depicting the vector velocity field.

3 Validation Campaign Description

In June and July 2007, a WindTracer system was deployed for a month-long campaign at a prospective wind farm site in the United States. The purpose of this effort was to collect volumetric wind data with the WindTracer, to process the data and retrieve vector velocities, and to compare those data to mast anemometer data. A cup-vane mast-mounted anemometer was set at a height of ~50 m and ~3.4 km away from the lidar.

A 10 minute, 16-tilt volume scan was utilized during these tests. This update time was longer than normal but afforded direct measurements between 70 and 90 meters above ground level (AGL) height at all viewable points within 6 km of the WindTracer. This limited the interpolation required in the vertical dimension.

4 Results

4.1 Vector Velocity Comparisons with a Mast Anemometer

Figure 6 shows a sample time-series comparison between the mast anemometer and the WindTracer. For the latter, an output point at the mast location and a height of ~50 m is extracted from the output grid of lidar-estimated volumetric data. Wind speed (upper) and wind direction (lower) estimates are compared. The mast anemometer data output was set to one minute updates while the lidar estimates were produced every 10 minutes, at the completion of each volume scan. This sample comparison extends for a 24-hour period and shows excellent agreement between the lidar and the anemometer.

Assessment of the lidar data accuracy is further quantified in Figure 7 through Figure 10. These figures plot the lidar-estimated parameter of interest against the corresponding mast-anemometer-estimated parameter. The full month-long data set is utilized and the anemometer data has now been averaged with a 10-minute wide sliding window filter. These figures correlate estimates of wind speed, wind direction, U-component, and V-component, respectively. A positive U-component velocity is to the East. A positive V-component velocity is to the North.

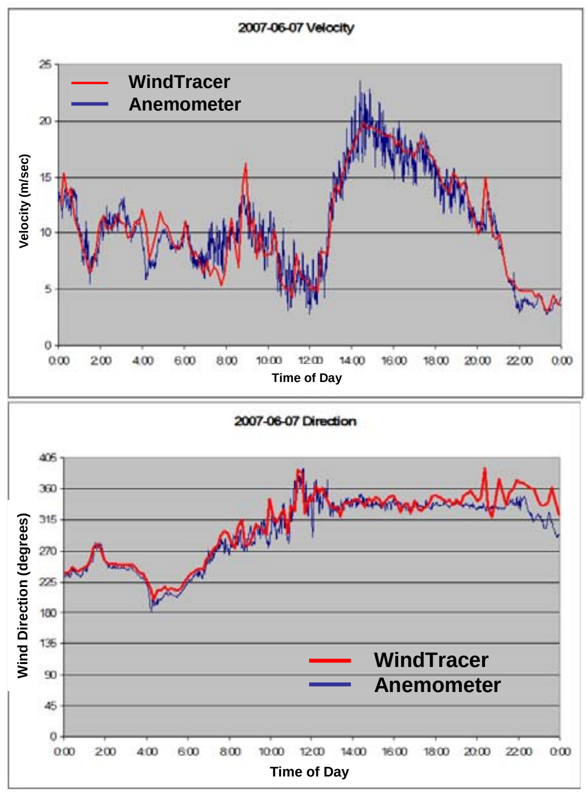

Figure 6: Sample vector wind measurement comparison between the LIDAR (thick/red) and a mast anemometer (thin/blue). The wind speed (upper) and wind direction (lower) are co-plotted for a 24-hour period on 7 June 2007. The anemometer data is updated once per minute as compared with the LIDAR data that is updated once every 10 minutes.

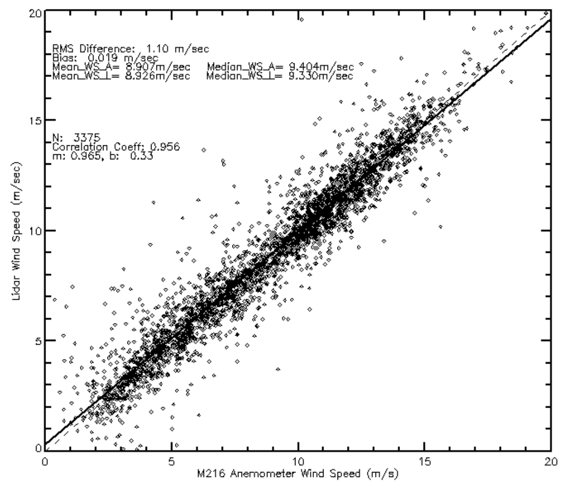

Figure 7: Wind speed correlation scatter plot of the lidar and mast anemometer month-long data sets. Standard regression analyses produced the best fit line, showing 96% correlation.

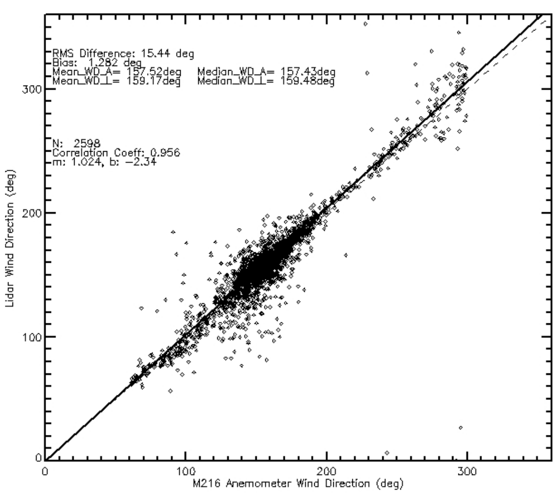

Figure 8: Wind direction correlation scatter plot of the lidar and mast anemometer month-long data sets. Standard regression analyses produced the best fit line, showing 96% correlation subject to wind speeds greater than 3 m/sec and directions between 60 and 300 degrees.

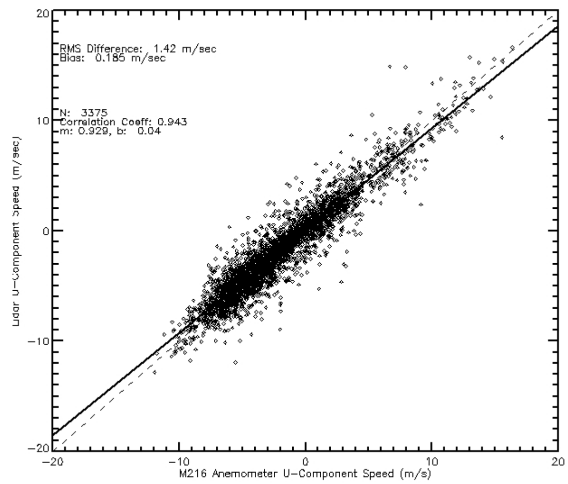

Figure 9: Correlation scatter plot of the lidar and anemometer data for the U-component of the wind speed.

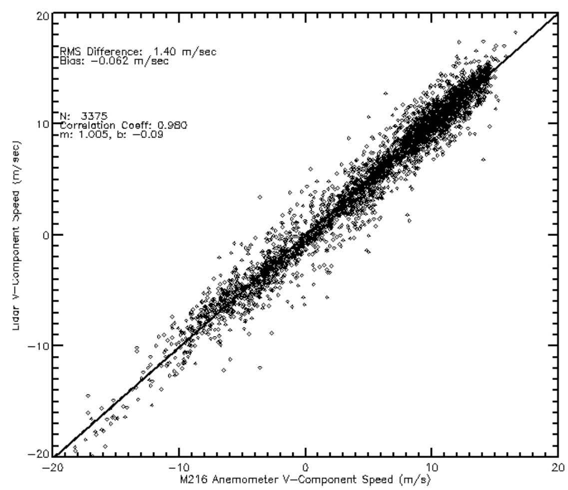

Figure 10: As above but for the V-component of the wind vector.

Table 2 summarizes the comparison results for wind speed and direction. The WindTracer and anemometer data are shown to agree quite well. Most remarkably, the month-long mean wind speed estimated by the lidar is shown to be *within 2 cm/sec* of the month-long mean wind speed estimated by the anemometer. This is an agreement that is within ~0.2%. The average wind direction agrees to 1.7 degrees, which is extraordinary considering the fidelity with which the mast anemometer alignment is typically performed.

Parameter	Met Mast	Lidar	Comparison
Wind Speed - mean - RMS*	 8.91 m/s 3.42 m/s	 8.93 m/s 3.50 m/s	Mean Diff: 0.02 m/s RMS Diff: 1.1 m/s Correlation: 96%
Wind Dir - mean*	 157.5°	 159.2°	Mean Diff: 1.7° RMS Diff: 15.4° Correlation: 96%

* conditioned on met mast speed >3 m/sec
** conditioned on above and direction 60-300 deg

Table 2: Summary of statistical comparison of wind speed and direction estimates between the mast anemometer and the lidar.

Figure 11 plots the probability density function of the wind speed over the month for the lidar and the mast anemometer. The agreement is quite good, and a bimodal distribution is evident. The lower mode is centered around 5 m/sec and the upper mode is just above 10 m/sec. The two density functions agree quite well. For anemometer-estimated wind speeds above 3 m/sec, the month-long RMS wind speed variability is 3.50 m/sec. The lidar data shows a comparable month-long RMS of 3.42 m/sec, within 2.3% of the anemometer's estimate.

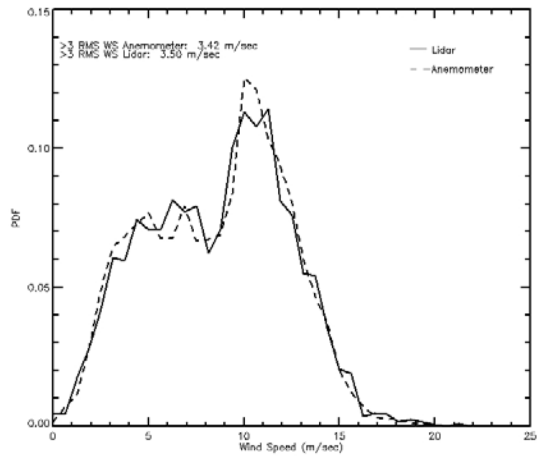

Figure 11: Probability density function of the wind speed at the mast anemometer location over the month-long data collection period. The solid line shows the lidar-estimated distribution and the dashed line is derived from the anemometer data.

4.2 Terrain-Following Wind Maps

One of the key objectives for the data collection campaign was to generate large-scale wind field maps at a user-selected height above ground. DEM data was utilized by the post-processing software to produce these types of results and data visualizations. Figure 12 shows the mean wind speed map for a constant AGL-height of 80 meters. This height is a typical hub height for modern-day wind turbines. This terrain-following wind speed map provides direct visualization of the mean winds over the site. Because the predominant wind direction is nominally out of the SSE (~157 degrees), the largest mean wind speeds are observed along the northern ridge of the mesa. On the top of the mesa, lower-lying areas (e.g., creek beds) indicate lower wind speeds, as expected. Additional data products that would be informative to display in a similar fashion include turbulent intensity, maximum wind speed, average wind direction, and so on.

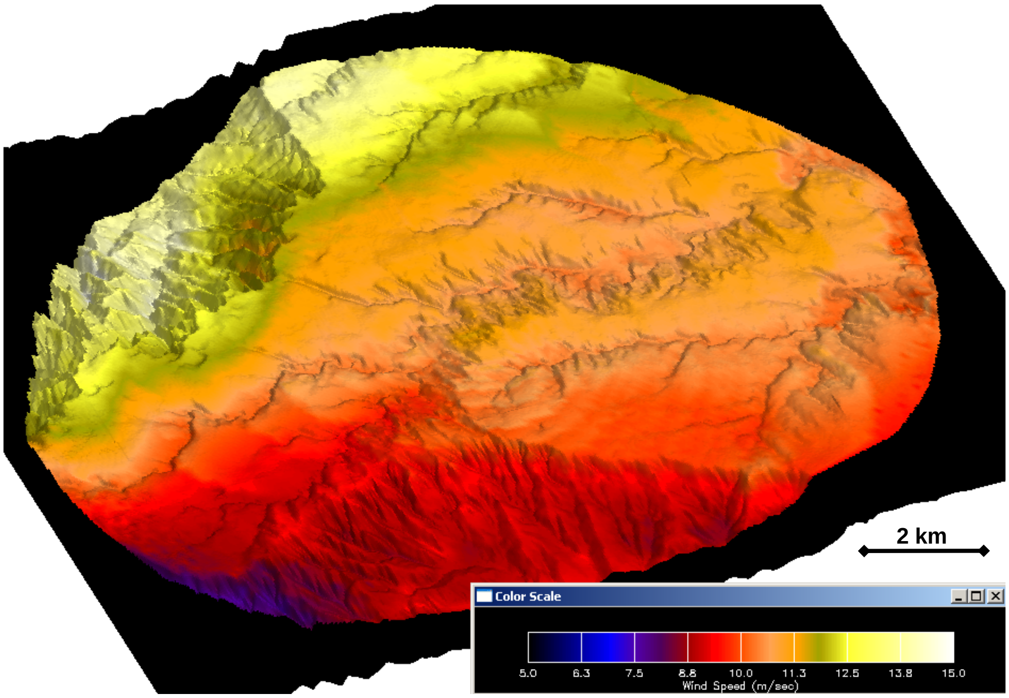

Figure 12 Terrain-following mean wind speed map at an AGL height of ~80 m, corresponding to a nominal hub height. The color-coded data is plotted as a texture map to depict the terrain. The vertical height scale has been accentuated to highlight the height variations in the terrain.

5 Summary

A month-long evaluation and validation campaign using a WindTracer pulsed Doppler lidar has been conducted. The WindTracer is presently in use at airports around the world and operates at eyesfe infrared wavelengths. This lidar provides significantly larger spatial coverage than sodar and emerging short-range lidar devices and would enable efficient wind resource characterization if the accuracy and representativeness of the data can be verified.

Comparison between the vector wind estimates produced by a mast anemometer and the lidar are quite good. Month-long mean wind speeds for this data set agree to within 2 cm/sec (0.2%). Wind probability density functions show similarly good agreement. Further characterization of the sensor performance is ongoing, including evaluation of more complex vector retrieval algorithms that can achieve higher output spatial resolution.

The gridded output data from the WindTracer has been coupled with DEM data to produce a unique terrain-following wind product map. Such maps would be very useful to wind prospecting and resource characterization activities. Direct observation of winds in this fashion can feed into micrositing of turbines and verification of model predictions. Measurements are made not only at hub height, but at user-defined heights that cover the full span of the turbine. Shear and turbulence effects, which are important contributors to fatigue load assessment, can be directly measured. Future application of the technology would also include larger-scale measurements of wind farm wake effects.

References

[1]. Shun, C. M., 2003: "Ongoing research in Hong Kong has led to improved wind shear and turbulence alerts," *ICAO J.*, November, 58, pp. 4-6 (2003).

[2]. Hannon, S. M., 2004: "Pulsed Doppler LIDAR for Terminal Area Monitoring of Wind and Wake Hazards," *Proc. 11th Conf. on Aviat., Range and Aerosp. Meteorol.*, 4-8 October 2005, Hyannis, Massachusetts.

[3]. S. M. Hannon, J. V. Pelk, S. R. Vetorino, "Next Generation Doppler Lidar Sensor at 1.6 μm," in Proceedings, 14th Coherent Laser Radar Conference, Snowmass Village, Colorado (2007).

[4]. P. W. Chan and A. M. Shao, "Two-dimensional Wind Retrieval Using a Doppler LIDAR," in *13th International Symposium for the Advancement of Boundary Layer Remote Sensing*, Garmisch-Partenkirchen, Germany, 18-20 July 2006.